Supplementary information for: Azimuthal beam shaping in orbital angular momentum basis

Zhongzheng Lin[1,*], Weihang Zhong[1,*], Lixun Wu[1], Lin He[1], Hongjia Chen[1], Jianqi Hu[2], Yujie Chen[1,†], Siyuan Yu[1,‡]

[1]State Key Laboratory of Optoelectronic Materials and Technologies, School of Electronics and Information Technology, Sun Yat-sen University, Guangzhou 510275, China.

[2]École Polytechnique Fédérale de Lausanne, Photonic Systems Laboratory (PHOSL), STI-IEM, Station 11, Lausanne CH-1015, Switzerland.

*These authors contributed equally to the work

†Yujie Chen, chenyj69@mail.sysu.edu.cn

‡Siyuan Yu, yusy@mail.sysu.edu.cn

Supplementary Note 1. Design of the phase masks

The proposed azimuthal shaping is based on multiple phase modulation, such that the phase masks loaded on the spatial light modulator (SLM) is the most significant. The phase masks can be divided into two parts, the phase masks that remain constant and are used to achieve OAM mode sorting, and the phase masks that change dynamically and are used for OAM mode spectrum modulation. In this supplementary note, we show how these phase masks are designed in detail. We describe the method for design of OAM mode sorter in section 1.1, and the dynamic phase mask for each functionality demonstration in section 1.2.

1.1 Design of the OAM mode sorter

As mentioned in the main text, the OAM modes are sorted in principle of multi-plane light conversion (MPLC). MPLC is a wavefront shaping technology that could transforming a set of orthogonal spatial modes into another using a sequence of phase masks separated by free space[23]. The phase distribution of the phase masks is determined in an inverse design process according to the input and output modes, and has no analytical expression. The algorithm for the inverse design is the

wavefront matching method, which iteratively optimizes each phase mask by compensating the phase mismatch between the input and output modes on its plane. In every iteration, the phase mask would be updated to[24]

$$\phi = \exp\left\{ i \arg\left[\sum_{i=1}^{N} (w_i f_i b_i^* \bar{\theta}_i) \right] \right\}, \tag{S1}$$

where N is the number of input modes (as well as the number of the output modes, and in our experiment $N = 17$), and f_i and b_i are the ith mode in the forward and backward direction, respectively. w_i is the weight of the ith pair of the modes and can be adjusted to balance the mode conversion efficiency between different modes. $\bar{\theta}_i$ is a constant phase and we take the average phase of $f_i b_i^*$. While MPLC is theoretically lossless and better results are generally obtained with more phase masks, the loss of actual device would increase if more phase masks are used. We choose to use 5 phase masks in order to balance the performance of mode conversion and the loss.

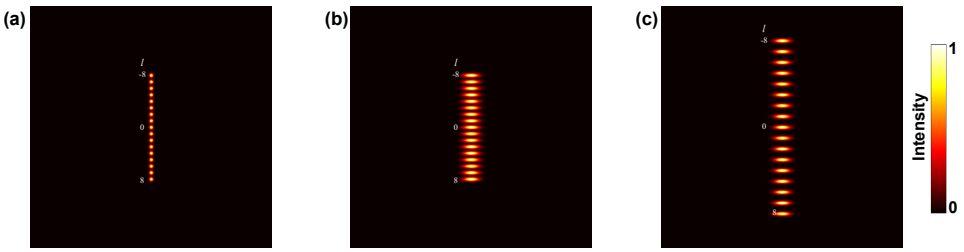

Fig S1 Different configurations for sorted beams. (a) Gaussian spots array with spacing of $150\,\mu m$. (b) Elliptical Gaussian spots array with spacing of $150\,\mu m$. (c) Elliptical Gaussian spots array with spacing of $300\,\mu m$.

The parameters of the output mode profile, including the shape of output spots and the spacing between adjacent spots, are determined through a trial-error process. Fig. S1 shows different configuration for the output mode profile, including 1) Gaussian spots array with moderate spacing ($150\,\mu m$), 2) elliptical Gaussian spots array with moderate spacing ($150\,\mu m$) and 3) elliptical Gaussian spots array with large spacing ($300\,\mu m$). The designed phase masks for each configura-

tion is shown in Fig. S2. Note that Fig. S2(b) is the same as Fig. 1(b) in the main text. It can be seen that the phase masks of configuration 2) is smoother than the others, which indicates higher tolerance for alignment errors. The mode conversion efficiency is also higher for configuration 2, as shown in Fig. S3. As a result, configuration 2) is chosen. Other parameters such as w_{0x}, w_{0y}, and the distance between phase masks are determined by a similar approach.

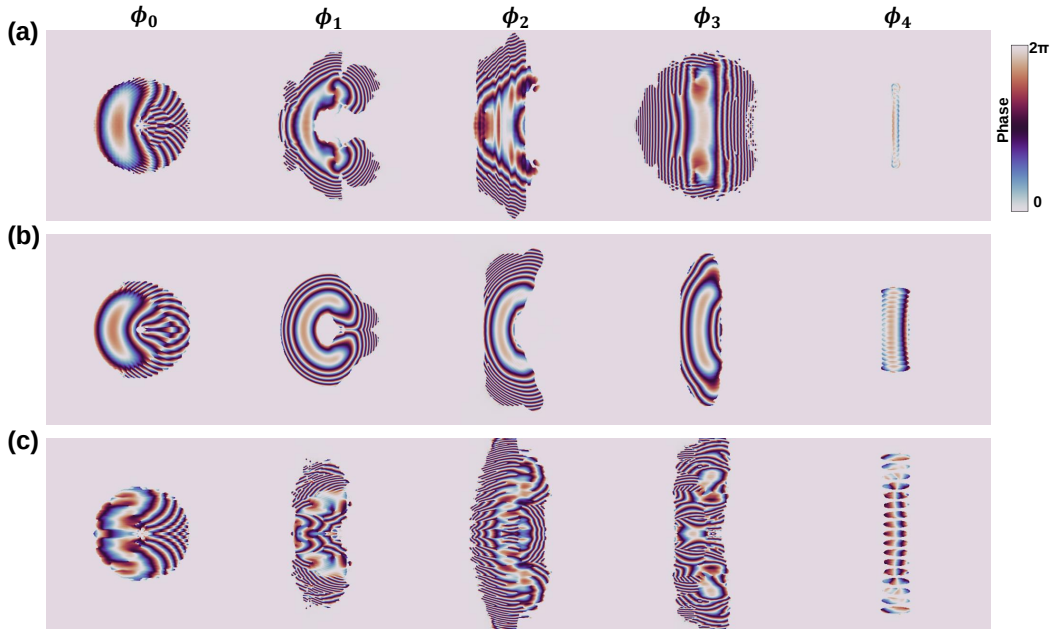

Fig S2 The inversely designed phase masks for different mode configurations. (a)-(c) corresponding to the configuration 1-3.

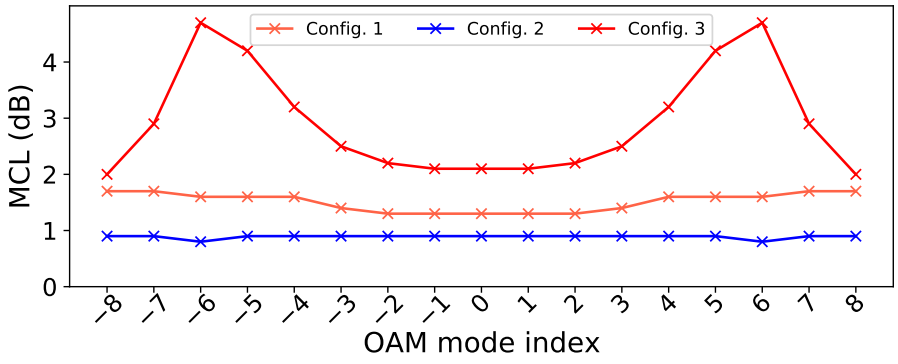

Fig S3 The mode conversion loss for different mode configurations.

1.2 Additional phase masks for functionality demonstration

As mentioned in the main text, except for phase for mode sorting and conjugation, additional phase would be applied in region R_5 for complex amplitude modulation of the OAM mode spectrum. In this section we describe additional phase for each functionality demonstration in detail.

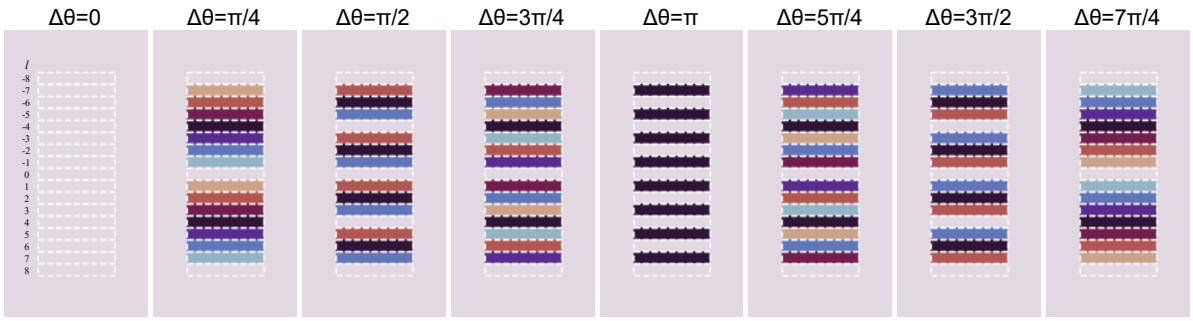

Fig S4 Linear spectral phase modulation $\psi_l = exp(i\ell\Delta\theta)$ for rotation of the beam.

For rotation of the beam, the linear spectral phase modulation can be expressed as

$$\psi_l = \exp(i\ell\Delta\theta), \tag{S2}$$

where ℓ refers to OAM mode order and $\Delta\theta$ refers to the rotation angle. Corresponding to Fig. 3 in the main text, the additional phase for different rotation angle is shown in Fig. S4.

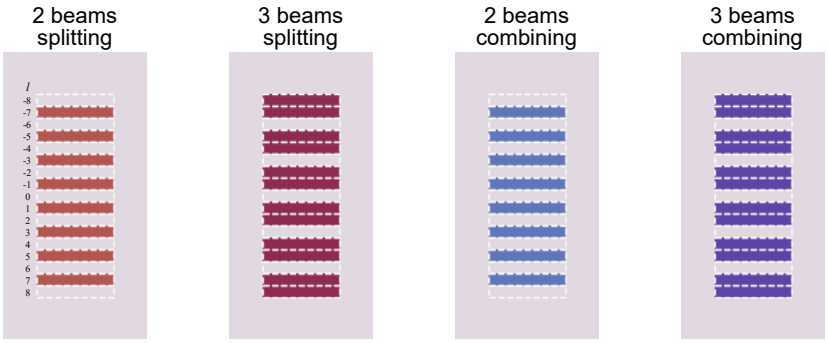

Fig S5 Talbot phase and its conjugate for beam splitting and combining.

The spectral phase modulation for azimuthal beam splitting and combining is the Talbot phase,

which is[17]

$$\psi_{l,N} = \begin{cases} \exp(i\frac{\pi l^2}{N}), & \text{if} \quad N \equiv 0 \pmod 2 \\ \exp(i\frac{2\pi l^2}{N}), & \text{if} \quad N \equiv 1 \pmod 2. \end{cases} \tag{S3}$$

where N represent the order of the splitting. The phase modulation for combination is the conjugate of Eq. S3. Corresponding to Fig. 4 in the main text, the phase modulation for beams splitting and combining is shown in Fig. S5.

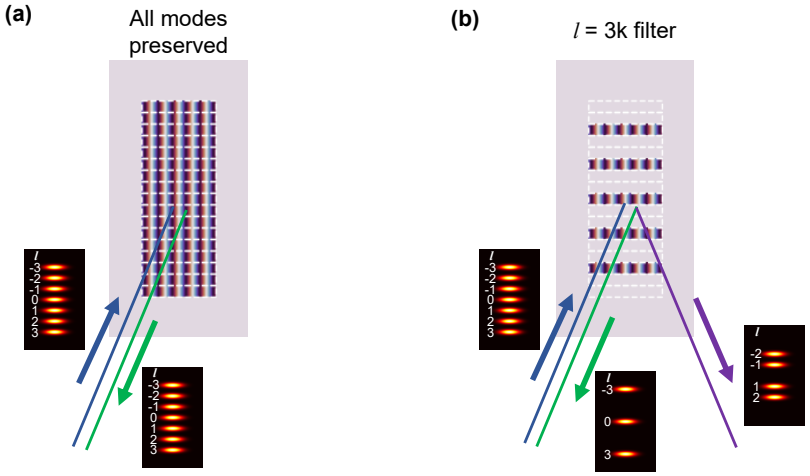

Fig S6 Localized linear phase grating for OAM modes filtering. (a) The grating covers all the sorted elliptical beams that all the OAM modes would reverse their propagation direction and be preserved. (b) The grating only assigned of OAM modes satisfying $\ell = 3k$, and the other modes would output from the other port and dissipate in the environment.

Besides spectral phase modulation, linear phase grating is used to control the amplitude of the OAM mode spectrum, which can be expressed as

$$\phi = \exp(ikx \sin\theta_g), \tag{S4}$$

where $k = 2\pi/\lambda$ represents the wave vector and θ_g represents the angle that the grating deflects the light. The θ_g of grating is designed to reverse the optical axis, so that the sorted elliptical beams can pass through the phase masks in backward direction and be recombined into co-axis

OAM modes. The grating is localized to only cover the desired OAM modes. By eliminating the grating, the unwanted OAM modes would be dropped from the other port and then dissipate into the environment. In Fig. S6(a), the grating covers all the sorted elliptical beams and all the OAM modes are preserved. It is the case when only spectral phase modulation is needed, such as above demonstration of beam rotation and sorting. In Fig. S6(b), the grating is localized only for OAM modes $\ell = 3k$, while the other modes being dropped.

Supplementary Note 2

As the structure and parameters of the azimuthal beam shaper have already been described in section 2.1 of the main text, this section provides an additional description of the experimental setup for demonstration and characterization of the azimuthal beam shaper.

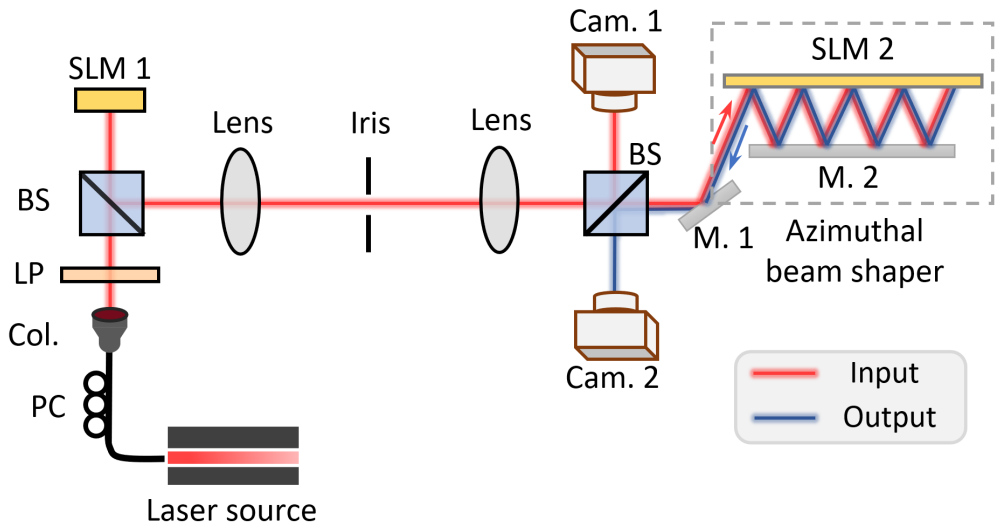

Fig S7 Experiment setup for demonstration and characterization of the azimuthal beam shaper. The azimuthal shaper is composed of SLM2 and mirror 2. Col.: collimator, BS: beam splitter, SLM: spatial light modulator, Cam.: camera, M.: mirror.

As shown in Fig. S7, the 1550 nm wavelength laser beam is first collimated and output into free space. The beam is then linearly polarized and incident to the phase-only SLM 1. Loading a special computer-generated hologram on the SLM 1 and in combination with a follow-up 4-f

system composed of a pair of 200 mm focal length lenses and a iris, OAM modes with specific mode spectrum are generated[26]. The generated OAM modes enter the azimuthal beam shaper (i. e. SLM 2 and mirror 2), and its intensity distribution is recorded by camera 1 via a beam splitter. After spectrum modulation, with the optical axis of beam reversed, the beam propagated backward and output from the same port as the input. The red line and blue line denote the light before and after optical axis reversal, respectively. The output beam is separated from the input through a beam splitter, with its intensity distribution captured by camera 2. Camera 1 was placed 35 cm behind the back focal plane of the 4-f system, and camera 2 and camera 1 are placed symmetrically with respect to the beam splitter. When demonstrating different azimuthal beam shaping, the phase masks loaded on the SLMs are switched. When characterizing the loss, the two cameras are replaced by power meters.

Since the beam is required to pass through the center of the phase mask on each reflection, and a specific propagation distance is desired between the two reflections, the azimuthal beam shaper is sensitive to alignment errors. The SLM and mirror each have six adjustable degrees of freedom, and each of them is finely tuned in order to obtain optimal performance, especially the parallelism between the SLM and mirror. The alignment can be further optimized by applying additional phase on the SLM to compensate its surface unevenness or using smoother phase masks designs that is more tolerant to the errors.